Arch. Metall. Mater. **65** (2020), 2, 721-726

DOI: 10.24425/amm.2020.132811

G. JUNAK[1*]

FATIGUE PROPERTIES OF AZ31 AND WE43 MAGNESIUM ALLOYS

The paper presents low-cycle fatigue (LCF) characteristics of selected magnesium alloys used, among others, in the automotive and aviation industries. The material for the research were bars of magnesium alloys AZ31 and WE43 after hot plastic working. Due to their application(s), these alloys should have good/suitable fatigue properties, first of all fatigue durability in a small number of cycles.

Low-cycle fatigue tests were carried out on the MTS-810 machine at room temperature. Low-cycle fatigue trials were conducted for three total strain ranges $\Delta\varepsilon_t$ of 0.8%, 1.0% and 1.2% with the cycle asymmetry factor $R = -1$. Based on the results obtained, fatigue life characteristics of materials, cyclic deformation characteristics $\sigma_a = f(N)$ and cyclic deformation characteristics of the tested alloys were developed. The tests have shown different behaviors of the tested alloys in the range of low number of cycles. The AZ31 magnesium alloy was characterized by greater fatigue life N_f compared to the WE43 alloy.

Keywords: low-cycle fatigue, mechanical properties, magnesium alloy

1. Introduction

Light metal alloys, including magnesium alloys such as AZ31 and WE43, are widely used in many industries, mainly in the automotive, machine, railway and aviation industries [1-4]. AZ31 magnesium alloy (EN-MAMgAl3Zn1) is characterized by good mechanical properties at a low price. It can be shaped in processes such as rolling, extrusion, and forging [5]. Its low density makes it an attractive material for the automotive industry [4].

WE43 (Mg-4Y-3RE) cast magnesium alloy containing yttrium and rare earth elements is intended for operation at 250°C, with acceptable short-term operation up to 300°C. This alloy is gravity cast in sand moulds, used for large-size castings that are used in the aviation industry [6,7]. The WE43 alloy also exhibits good mechanical properties and high corrosion resistance.

Wrought magnesium alloys were used sporadically, which resulted from technological difficulties in the plastic working and high production costs. Low deformability of magnesium alloys at temperatures up to 200°C resulted from a limited number of slip systems in the hexagonal crystal network [8,9]. The mechanical properties of magnesium alloys after plastic working are higher compared to foundry alloys [4]. The most advantageous set of properties have alloys from the Mg-Al-Zn-Mn group, containing up to 8% Al with the addition of Mn (up to 2%), Zn (up to 1.5%) [1,10,11].

2. Material and research methodology

The material for testing included two sets of rods: alloy AZ31 rods with 20 mm diameter after extrusion and annealing at 400°C with a heating time of 60 minutes with subsequent cooling in the air, and rods of WE43 alloy with 20 mm diameter in a hot-pressed condition. The microstructures of the tested materials are shown in Fig. 1.

The chemical compositions (Tab. 1) and the basic mechanical properties of the tested alloys determined on the basis of a static tensile test at room temperature (Fig. 2) are summarized in Table 2. AZ31 magnesium alloy compared to WE43 alloy had a much lower conventional yield point $R_{p0.2}$ determined in the compression test (Fig. 3).

Low-cycle fatigue tests were carried out at room temperature on an MTS-810 testing machine using the TestSTAR II and TestWARE SX software. The tests were carried out in conditions including uniaxial stretching and compression with the value of cycle asymmetry factor $R = -1$, for three total strain ranges $\Delta\varepsilon_t$ equal to 0.8%, 1.0% and 1.2%. Threaded cylindrical samples with a measuring base of 12 mm diameter and 32 mm length were used in the tests.

[1] SILESIAN UNIVERSITY OF TECHNOLOGY, INSTITUTE OF MATERIALS ENGINEERING, 8 KRASIŃSKIEGO STR., 40-019 KATOWICE, POLAND

* Corresponding author: grzegorz.junak@polsl.pl

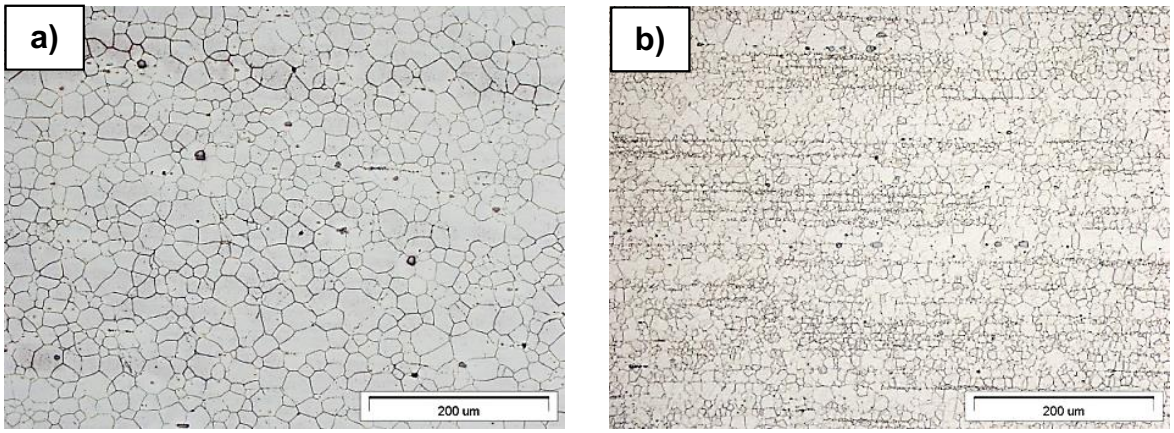

Fig. 1. Fine-grained microstructure of magnesium alloys: a) AZ31 alloy, b) WE43 alloy

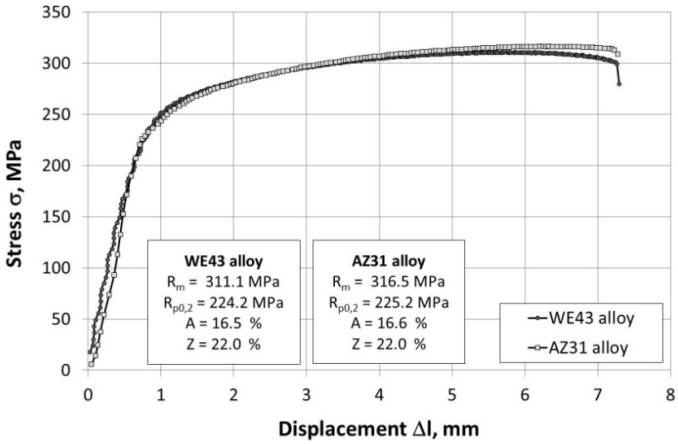

Fig. 2. Static tensile tests curves of tested AZ31 and WE43 alloys

TABLE 1

Chemical composition of tested AZ31 and WE43 alloys

AZ31 alloy							
Al	**Cu**	**Fe**	**Mn**	**Ni**	**Si**	**Zn**	**Mg**
2.5-3.5	0.05	0.01	0.15-0.4	0.01	0.1	0.6-1.4	others
WE43 alloy							
Y	**Nd**	**RE**	**Zr**	**Mn max.**	**Cu max.**	**Ni max.**	**Zn max.**	**Mg**
4	2.0	3.4	min. 0.4	0.15	0.03	0.005	0.2	others

TABLE 2

Main mechanical properties of tested AZ31 and WE43 alloys

Alloy	**Main mechanical properties**				
	R_m **(UTS), MPa**	$R_{p0.2}$ **(YS), MPa**	A**, %**	Z**, %**	E**, GPa**
AZ31	316.5	225.2	16.6	22.0	43.7
WE43	311.1	224.2	16.5	22.0	42.8

3. Test results

In the course of the fatigue test, changes in the value of loading, displacement and deformation of the sample were continuously recorded in time using an extensometer with a measuring base of 25 mm. Based on these data, hysteresis loops for half the number of cycles to failure were developed for individual ranges of total deformation $\Delta\varepsilon_t$ (Figs. 4 and 5).

Basic fatigue characteristics of the tested alloys were also developed including the characteristics of fatigue life in the form of the relationship $N_f = f(\Delta\varepsilon_t)$ shown in Fig. 6 and 7.

Fatigue life curves determined by the equation given by R.W. Smith, N.H. Hirschberg and S.S. Manson [13] are shown in Figures 8a and 8b.

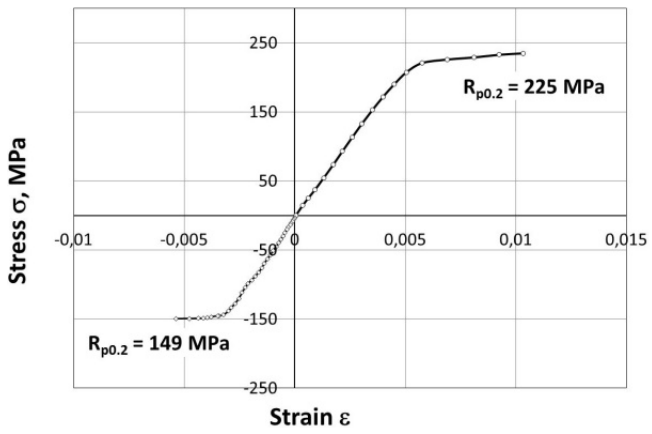

Fig. 3a. Static tensile and compression test curves of magnesium alloy AZ31[12]

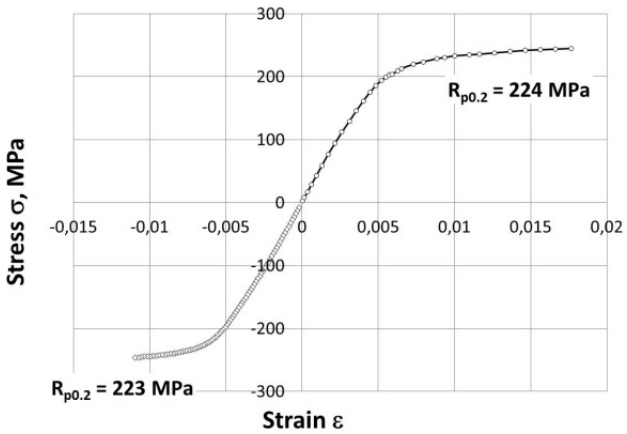

Fig. 3b. Static tensile and compression test curves of magnesium alloy WE43

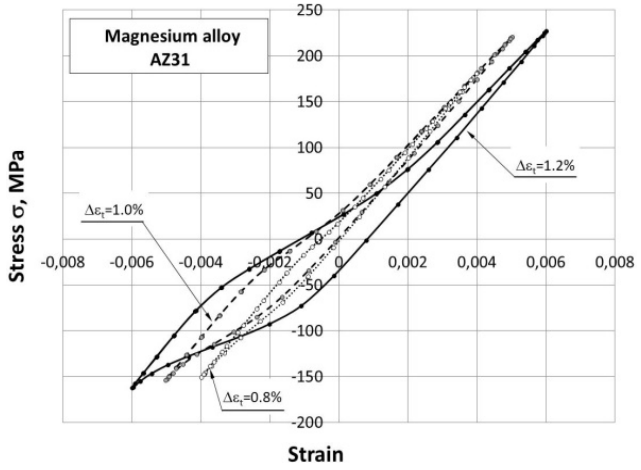

Fatigue process parameters (LCF)				Fatigue life N_f cycles
Strain range			Stress amplitude	
Total $\Delta\varepsilon_t$	Plastic $\Delta\varepsilon_p$	Elastic $\Delta\varepsilon_e$	σ_a, MPa	
0.008	0.00074	0.00726	176	7748
0.010	0.00142	0.00858	219	3098
0.012	0.00288	0.00912	225	664

Fig. 4. Hysteresis loops parameters determined for a half of the number of cycles to failure of magnesium alloy AZ31 [12]

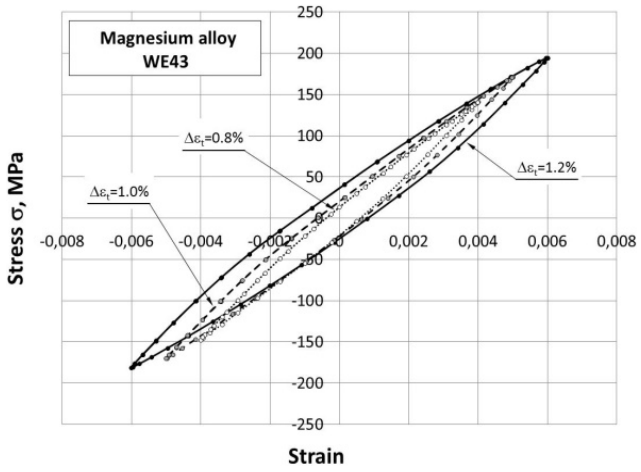

Fatigue process parameters (LCF)				Fatigue life N_f cycles
Strain range			Stress amplitude	
Total $\Delta\varepsilon_t$	Plastic $\Delta\varepsilon_p$	Elastic $\Delta\varepsilon_e$	ε_a, MPa	
0.008	0.00093	0.00706	144	3420
0.010	0.00135	0.00864	170	1770
0.012	0.00205	0.00994	188	320

Fig. 5. Hysteresis loops parameters determined for a half of the number of cycles to failure of magnesium alloy WE43

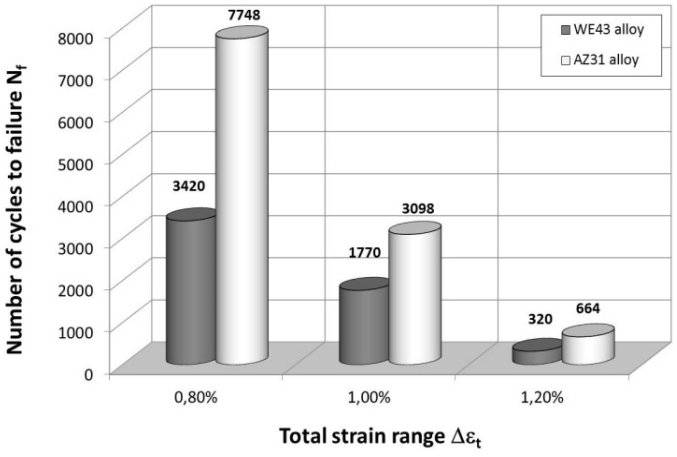

Fig. 6. Characteristics of fatigue life of the tested alloys

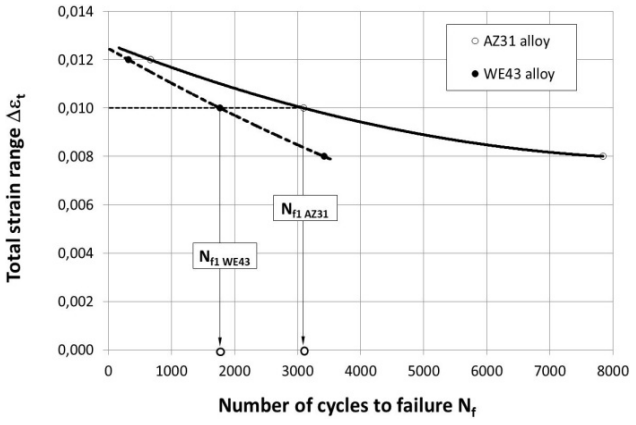

Fig. 7. Characteristics of fatigue life of the tested alloys in the form of dependence $N_f = f(\Delta\varepsilon_t)$

Waveforms for change in stress amplitude σ_a in low-cycle fatigue were developed in the form of cyclic deformation characteristics $\sigma_a = f(N)$ (Fig. 9a and 9b) and cyclic deformation characteristics against the background of a static tensile test (Figs 10a and 10b) described by the formula $\sigma_a = K'(\varepsilon_{ap})^{n'}$ given by J.D. Morrow [13].

4. Analysis of test results

Tests carried out on AZ31 and WE43 magnesium alloys (Fig. 2, Tab. 2) showed similar values of basic mechanical properties determined on the basis of static tensile tests at room temperature, including both strength (R_m, $R_{p0.2}$, E) and plastic

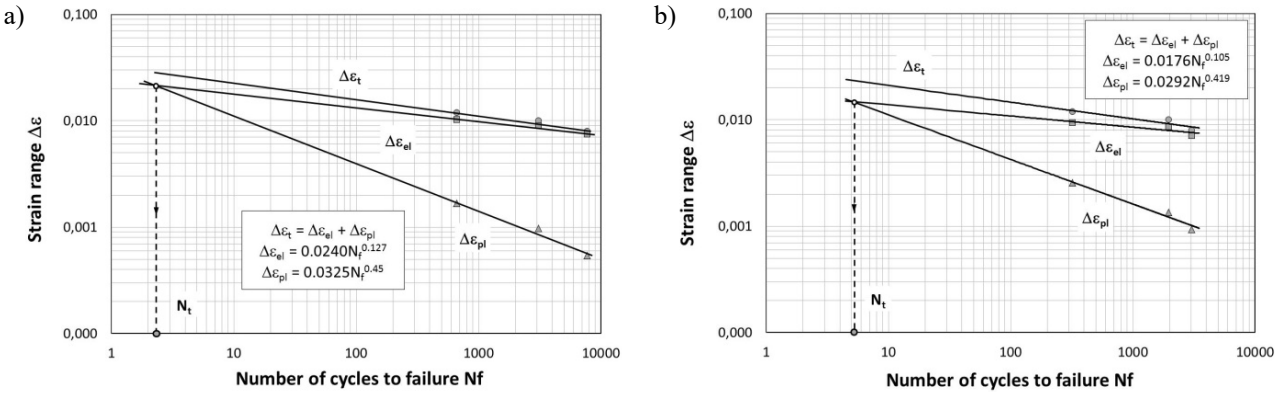

Fig. 8. Characteristics of fatigue life of magnesium alloys: a) AZ31 and b) WE43

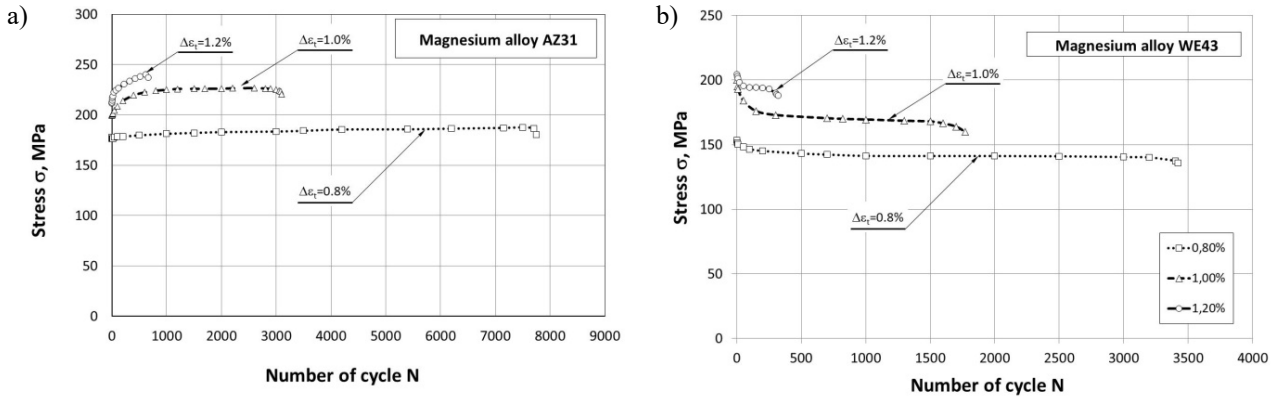

Fig. 9. Characteristics of cyclic deformation of magnesium alloys: a) AZ31, b)WE43

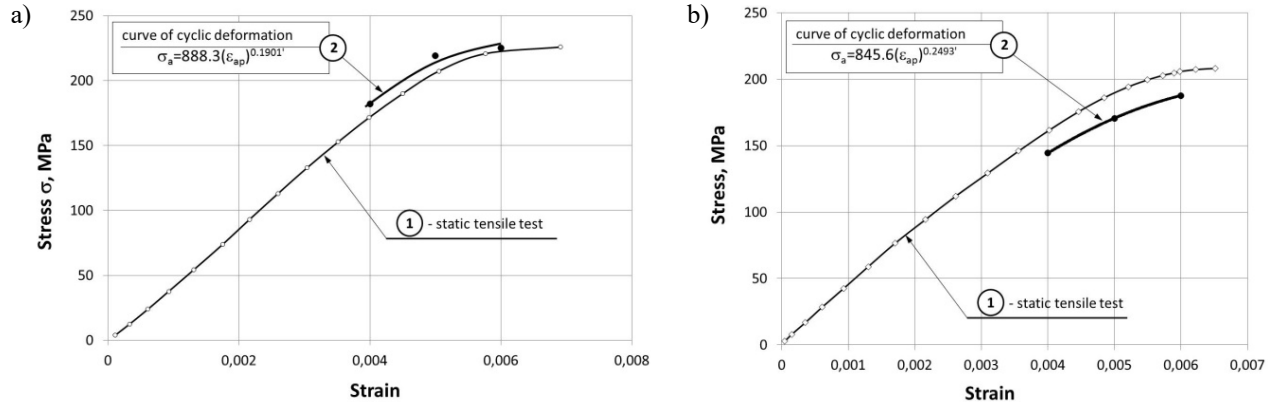

Fig. 10. Characteristics of cyclic deformation of magnesium alloys against the background of the static tensile test curve: a) AZ31, b) WE43

(A and Z) properties. However, based on the compression test (Fig. 3), AZ31 alloy exhibited a significantly lower yield strength value (by 33%) in relation to $R_{p0.2}$ = 223 MPa determined for WE43 alloy.

The analysis of fatigue characteristics developed for AZ31 alloy shows their significant differences compared to those determined for WE43 alloy.

In the low-cycle fatigue, classic symmetrical hysteresis loops were recorded for WE43 alloy, whereas for AZ31 alloy their shape showed anomalies manifested both in the lack of loop symmetry and in the values of the stress amplitude σ_a in tensile and compressive stress ranges (Figs. 4, 5). The observed anomalies in the shape of the hysteresis loop of AZ31 alloy with a compact hexagonal structure subjected to strong plastic processing in the production process show a strong fibrous texture. This results in anisotropic behavior of the material under tensile and compressive loading, oriented parallel to the extrusion direction. As a result, the samples subjected to variable tensile and compressive loading in the fatigue test show anomalies known as SDE (strength differential effect [1]).

The surface area under the characteristic determined in the static tensile test illustrates the accumulated damage energy at a level which causes the destruction of the material. It follows (Fig. 2) that strain values for both analyzed magnesium alloys

should be comparable. Assuming on the basis of the relationship (1) that the total accumulated damage energy (W_t) is the sum of damage energy at individual stages (W_n), and bearing in mind the results of the durability of individual alloys obtained at a specific level of total deformation $\Delta\varepsilon_t$ in low-cycle fatigue tests (Fig. 4 and Fig. 5), it could be expected that the damage energy determined for a single hysteresis loop should be almost twice as high for the WE43 alloy (due to the number of cycles to failure).

$$W_t = \sum_{i=1}^{n} W_n \tag{1}$$

The analysis of the stabilized hysteresis loops, however, indicates that the damage energy for the WE43 alloy is 20% higher than that determined for the AZ31 alloy (Fig. 11).

Alloy	Damage energy value, J
AZ31	2.06
WE43	2.47

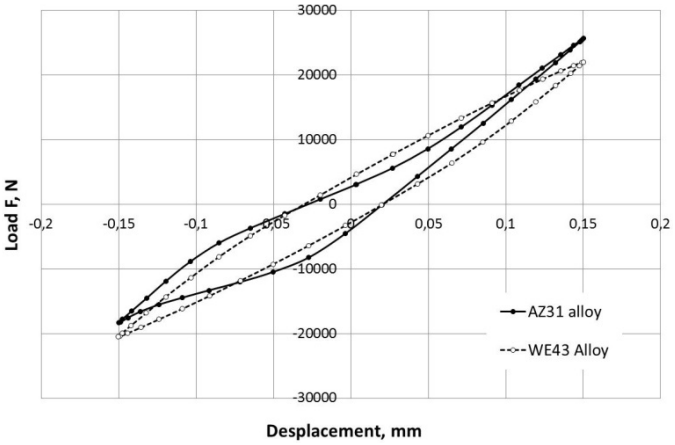

Fig. 11. Hysteresis loops parameters determined for a half of the number of cycles to failure of WE43 and AZ31magnesium alloys ($\Delta\varepsilon_t$ =1.2%)

The main cause of the damage to materials due to low-cycle fatigue is the value of the range of plastic deformation $\Delta\varepsilon_p$. With WE43 alloy, we obtain a classic hysteresis loop in tests (the maximum value of the plastic deformation range occurs at zero stress level, the loop showing a symmetric stress transfer). However, anomalies in both the shape and the symmetry of stress transmission were recorded for the AZ31 alloy (Fig. 4). The value of the maximum tensile stress recorded for the total strain range $\Delta\varepsilon_t$ = 1.2% was 226.8 MPa, while the value of the compressive stress was merely –162.2 MPa. It might therefore be concluded that the maximum range of plastic deformation does not occur at zero stress level, but is shifted towards compressive stresses of about –72.8 MPa. The values of individual ranges of plastic deformation of AZ31 with stress levels at 0 and –72.8 MPa (the latter being its maximum value), are shown in Fig. 12.

It follows that the maximum observed range of plastic deformation ($\Delta\varepsilon_p$ = 0.00288) is almost 60% higher than the level of plastic deformation recorded at zero stress level.

AZ31 alloy $\Delta\varepsilon_t$ = 0.012	
$\Delta\varepsilon_{p1}$	0.00181
$\Delta\varepsilon_{p2}$	0.00288

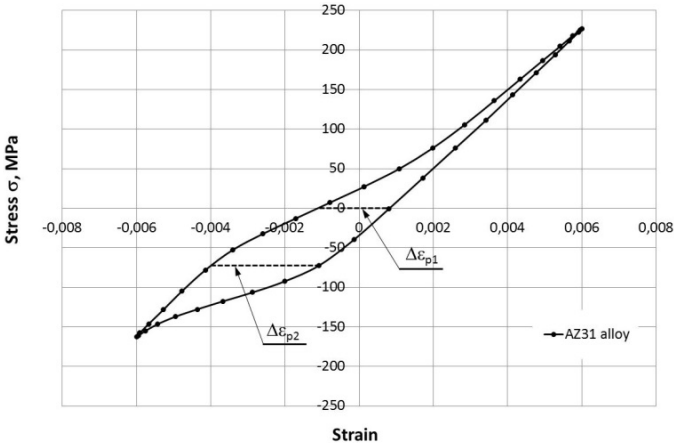

Fig. 12. Range of plastic deformation of AZ31 alloy in stabilized state ($\Delta\varepsilon_t$ =1.2%)

Anomalies in the shape and symmetry of the AZ31 hysteresis loop also show a much higher proportion of damage energy in compressive stress where it is about 63% of the damage energy per single hysteresis loop, which may be the cause of a much higher fatigue life understood as the number of cycles to failure as compared to WE43 alloy. In the case of WE43 alloy, no such behavior was recorded, the value of damage energy for tensile and compressive stresses was comparable in this test.

In the conducted fatigue tests, the N_f durability of AZ31 Mg alloy expressed in the number of cycles to crack initiation was significantly – about twice – higher for individual total strain ranges $\Delta\varepsilon_t$ than the low-cycle durability of WE43 alloy (Figs. 6 and 7).

The analysis of deformation characteristics as a function of the number of cycles to destruction (Fig. 8) indicates that the intersection of lines $\Delta\varepsilon_{el}$ and $\Delta\varepsilon_{pl}$ is in the area of a small number of cycles for both AZ31 (N_t = 2) and WE43 (N_t = 5). Thus, the low-cycle fatigue of the materials took place with the dominant share of the elastic component of the strain range $\Delta\varepsilon_{el}$. At the same time, the low N_t value indicates that the low-cycle fatigue life of the alloys tested was primarily determined by strength properties. Among other things, the grain boundary cohesion in the polycrystalline microstructure of the examined magnesium alloys could be a factor determining their resistance to cyclic deformation. This is confirmed by fractographic fatigue crack studies. Only WE43 alloy, characterized by lower low-cycle durability, exhibited numerous secondary fatigue cracks along grain boundaries in the fatigue zone of the fracture (Fig. 13), which indicates their low cohesion.

Under fatigue testing, WE43 Mg alloy exhibited cyclical weakening, while AZ31 alloy showed cyclical strengthening (Fig. 9). The observed property of each alloy is confirmed by the position of the cyclic deformation characteristics $\sigma_a = K'(\varepsilon_{ap})^n$ against the background of the static load test curve (Fig. 10). The cyclic deformation characteristics of WE43 alloy are located

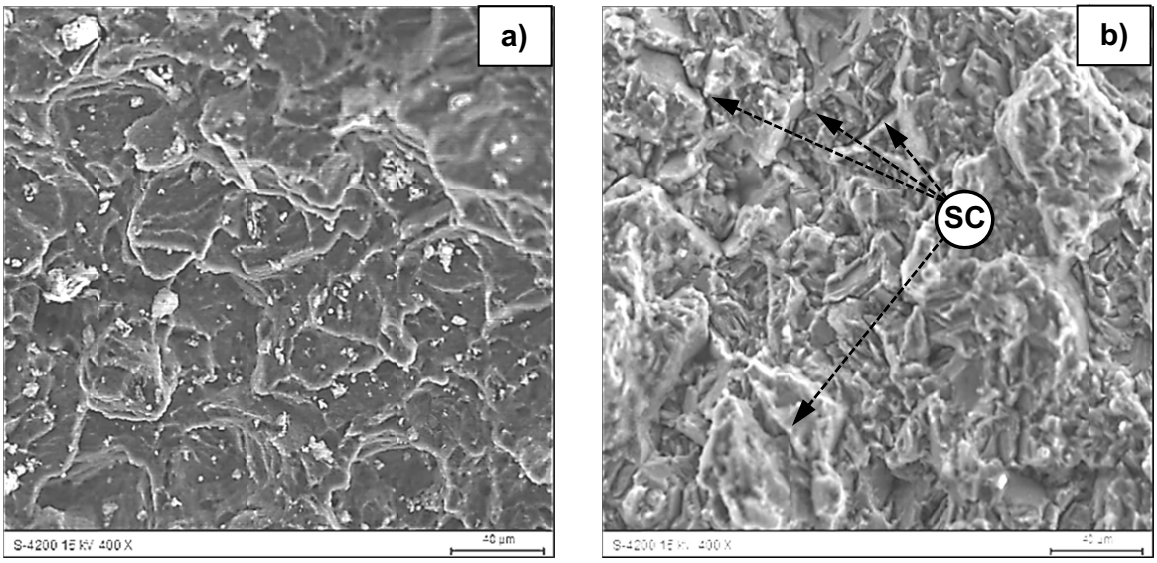

Fig. 13. Morphology of the fatigue zone after LCF tests: a) AZ31 alloy, b) WE43 alloy. SC – secondary cracks

below the static tensile curve, which indicates a weakening of materials. However, with AZ31 alloy, this characteristic lies above the static tensile strength characteristics, which is the result of a strengthening the material.

5. Summary

To sum up, it can be concluded that AZ31 magnesium alloy has a greater capacity for applications in conditions of variable elastic-plastic loads. Its fatigue life is nearly twice that of WE43 alloy, although its stress amplitude sa during LCF tests is about 30MPa higher compared to WE43 alloy. Much greater fatigue life of AZ31 alloy compared to WE43 alloy can be linked with anomalies in the shape of a hysteresis loop, which entails a different mechanism of nucleation and development of fatigue cracks. However, verification of this hypothesis requires further research.

REFERENCES

[1] K.E. Oczoś, A. Kawalec, Forming Light Metals, PWN, Warsaw (2012).

[2] Z. Pater, J. Tomczak, T. Bulzak, Numerical Analysis of Helical Rolling of a Hollow Roller Made of Titanium Alloy Ti6Al4V, Hutnik – Wiadomości Hutnicze, **82** (9), 599-603, (2015).

[3] J. Tao, Y. Zhang, F. Fan, Q. Cheen, Microstructural Evolution and Mechanical Properties of AZ31Magnesium Alloy Prepared by Casting-solid Extrusion Forging During Partial Remelting, Defence Technology **9**, 146-152, (2013).

[4] I. Schindler, P. Kawulok, E. Hadasik, D. Kuc, Activation energy in hot forming and recrystallization models for magnesium alloy AZ31, Journal of Materials Engineering and Performance **22** (3), 890-897, (2013).

[5] K. Drozdowski, K. Horzelska, Wpływ warunków kucia na strukturę stopów magnezu gatunku AZ 31 i AZ61 (The Influence of Forging Conditions on the Structure of Magnesium Alloys Grade AZ 31 and AZ 61), Hutnik – Wiadomości Hutnicze **82** (8), 488-493, (2015).

[6] A. Kiełbus, The influence of solution treatment time on the microstructure of WE43 magnesium alloy, Acta Metallurgica Slovaca **13**, 653-657, (2007).

[7] Elektron WE-43, Data sheet 467. Magnesium Elektron, Wielka Brytania (2006).

[8] S. Rusz, L. Cizek, J. Kedron, S. Tylsar, M. Salajka, E. Hadasik, T. Donič, Structure and Mechanical Properties Selected Magnesium – Zirconium Alloys, In Journal of Trends in the Development of Machinery and Associated Technology **16** (1), 55-58, ISSN 2303-4009, (2012).

[9] A.G. Beer, M.G. Barnett, Microstructure evolution in hot worked and annealed magnesium alloy AZ31, Material Science and Engineering A **485**, 318-324, (2008).

[10] F. Lv, F. Yang, Q.Q. Duan, Y.S. Yang, S.D. Wu, S.X. Li, Z.F. Zhang, Fatigue properties of rolled magnesium alloy (AZ31) sheet: Influence of specimen orientation, International Journal of Fatigue, 672-682, (2011).

[11] W. Kim, Y. Sa, Scripta Materialia **54**, 1391-1395 (2006).

[12] G. Junak, Low-cycle fatigue characteristics of selected titanium, magnesium and aluminium alloys Arch. Metall. Mater. **63** (4), 1949-1955, (2018).

[13] S. Kocańda, Zmęczeniowe niszczenie metali, WNT, Warszawa (1978).